Heavy Vehicles on Minor Highway Bridges

dynamic modelling of vehicles and bridges

Kirkegaard, Poul Henning; Nielsen, Søren R. K.; Enevoldsen, I.

Publication date:
1997

Document Version
Early version, also known as pre-print

INSTITUTTET FOR BYGNINGSTEKNIK
DEPT. OF BUILDING TECHNOLOGY AND STRUCTURAL ENGINEERING
AALBORG UNIVERSITET • AAU • AALBORG • DANMARK

STRUCTURAL RELIABILITY THEORY
PAPER NO. 171

P. H. KIRKEGAARD, S.R.K. NIELSEN, I. ENEVOLDSEN
HEAVY VEHICLES ON MINOR HIGHWAY BRIDGES - DYNAMIC MODELLING OF VEHICLES AND BRIDGES
DECEMBER 1997 ISSN 1395-7953 R9721

The STRUCTURAL RELIABILITY THEORY papers are issued for early dissemination of research results from the Structural Reliability Group at the Department of Building Technology and Structural Engineering, University of Aalborg. These papers are generally submitted to scientific meetings, conferences or journals and should therefore not be widely distributed. Whenever possible reference should be given to the final publications (proceedings, journals, etc.) and not to the Structural Reliability Theory papers.

Printed at Aalborg University

INSTITUTTET FOR BYGNINGSTEKNIK
DEPT. OF BUILDING TECHNOLOGY AND STRUCTURAL ENGINEERING
AALBORG UNIVERSITET • AAU • AALBORG • DANMARK

STRUCTURAL RELIABILITY THEORY
PAPER NO. 171

P. H. KIRKEGAARD, S.R.K. NIELSEN, I. ENEVOLDSEN
HEAVY VEHICLES ON MINOR HIGHWAY BRIDGES - DYNAMIC MODELLING OF VEHICLES AND BRIDGES

DECEMBER 1997 ISSN 1395-7953 R9721

CONTENTS

1. INTRODUCTION

Vibration of a bridge structure due to the passage of vehicles is an important consideration in the design of bridges. Further, a common problem in bridge engineering practice in these years is the upgrading of minor highway bridges (≈5-20 m) to carry heavier loads partly due to a tendency of heavier trucks moving at larger speeds, and partly because the authorities want to permit transportation of special heavy goods at a larger part of the road net. These needs will in many cases cause that strengthening of the bridges becomes necessary. In order to keep the expenses of such strengthening projects at a minimum, it is necessary to perform accurate estimates of the dynamic amplification factor (defined as the dynamic load effect divided by the static load effect from the vehicles), so this quantity is neither over- nor underestimated.

For the minor highway bridges the critical design scenario occurs at the simultaneous passage of two heavy vehicles. According to the present Danish regulations these two heavy vehicles are taken as a 50 t and a heavier 100 - 150 t vehicle, Vejdirektoratet (1996). For both these vehicles the dynamic amplification factor is taken simultaneously as 1.25, which is an expensive generalization for the strengthening projects, and underlines the need for better estimation and more bridge specific determination of the dynamic amplification factor.

The principal aims of the present paper are to establish the numerical models for the mathematical models of the vehicles and the bridge from which the load amplification factors can be estimated assuming that the dynamic parameters of the vehicles and the modal parameters of the bridge are known. The vehicles may move in the same or in opposite directions, may enter the bridge at different instants of time or at different speeds. The lightweight vehicle consists of a 48 t Scania 3 axle tractor and a 3 axle trailer, jointed in a flexible hinge. Each axle is suspended on two elastic supports modelling the wheels. Further, support springs are supplied between the axle and the superstructure, modelling the suspension system of the vehicle. The heavyweight vehicle is taken as a 106t Goldhofer truck, with a 3 axle tractor and a 8 axle trailer, consisting of sub-vehicles jointed together in unflexible hinges. The dynamic response of the bridge is assumed rather insignificant for the present shortspan bridge. For this reason a truncated normal mode expansion is used, which preserves the basic quasi-static response of the bridge, and includes the dynamic response of the few lowest eigenmodes.

2. DESCRIPTION OF VEHICLES AND BRIDGE

The simulation model is based on simultaneous passage of two heavy vehicles on a typical Danish minor highway bridge. In the following the specifications of the vehicles and the bridge are given.

2.1 Description of the Vehicles

The heavy vehicles are a standard Scania heavy lorry (~ 48 t.) and a Goldhofer SKPH 8 special transportation (~106 t). These types of vehicles are chosen since they are some of the most common heavy vehicles in Denmark.

2.1.1 Description of the Scania Heavy Lorry

A Scania heavy lorry was chosen as the lightweight vehicle in the project. The Scania , see figure 2.1 consists of two modules, a truck-tractor and a trailer. The truck-tractor has three axles and the trailer 3 axles.

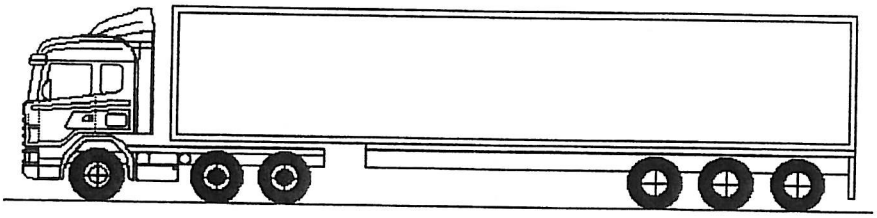

Figure 2.1 *A Scania heavy vehicle*

The Scania considered in the present study has the specifications given in table 2.1. (weight), table 2.2 (dimensions) and table 2.3 (axle load). These data are based on information from Ole M. Jørgensen, Scania Denmark.

Payload	Dead Weight	Gross Vehicle Load
kg	*kg*	*kg*
33839	14161	48000

Table 2.1 *Weight of the Scania vehicle.*

Width	Total Vehicle Length	Axle Spacing Tractor	Axle Spacing Trailer
m	m	m	m
2	16.5	2.35, 3.7	1.56

Table 2.2 *Dimension of the Scania vehicle.*

Tractor front	Tractor rear	5th Wheel Load	Trailer Axle Load
kg	*kg*	*kg*	*kg*
5249	9446, 9446	*17642*	*7953*

Table 2.3 *Axle load for the Scania vehicle.*

Based on the information from Scania the tractor has leaf springs in the front and air springs in the rear. No information about the trailer has been given, wherefore the trailer is assumed to have leaf springs. All wheels of the vehicle are assumed to have 295/80R22.5 tyres.

2.1.2 Description of the Goldhofer SKPH 8 Special Transportation

A 106 t Goldhofer SKPH 8 semi low loader vehicle is selected as the heavy special transportation vehicle. The Goldhofer SKPH 8, see figure 2.2 consists of two modules, a truck-tractor and a trailer. The truck-tractor has 3 axles and the trailer 8 axles.The heavyweight trailer consists of 8 sub-vehicles jointed together in unflexible hinges.

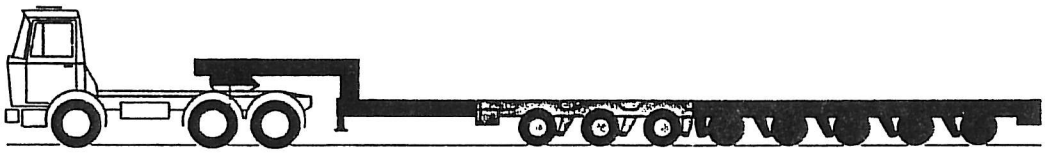

Figure 2.2 *A Goldhofer SKPH 8 .*

The Goldhofer SKPH 8 considered in the present study has the specifications given in table 2.4, (weight), table 2.5 (dimensions) and table 2.6 (axle load). These data are based on information from a Goldhofer brochure. However, the axle load for the tractor is estimated assuming a tractor with the same weight and load distribution as the Scania tractor in table 2.30

Speed	Payload	Dead Weight	Gross Weight	Gross Vehicle Load
km/h	*kg*	*kg*	*kg*	*kg*
62	70500	27000	97500	106000

Table 2.4 *Weight of the SKPH 8.*

Width	Total Vehicle Length	Loading Height	Axle Spacing Tractor	Axle Spacing Trailer
m	m	m	m	m
2.75	2.19	0.985±0.150	2.75 , 4.1	1.36

Table 2.5 *Dimension of the SKPH 8.*

Speed	Tractor Front	Tractor Rear	Axle Load	5th Wheel Load
km/h	*kg*	*kg*	*kg*	*kg*
62	5142	10429,10429	8x10000	17500

Table 2.6 *Axle load for the SKPH 8.*

The Goldhofer SKPH 8 has a wide variety of standard equipment for steering and loading, such as:

• In conjunction with the hydraulic axle compensation unit the hydraulical lift- and lowerable *Goose-neck* allows lifting/lowering of the loading platform, i.e. a constant static loading of the tractor fifth wheel on uneven roads.

• A hydraulic axle compensation (± 150 mm) incorporating hydraulic cylinders with swivel bearings, ensures a minimum wear .

The SKPH 8 considered in this study is assumed to have axle compensation units at the bogies of the semi lowloader., i.e at all of the eight axles.

The axle compensation units at the bogies is effected by cylinders in vertical arrangement in the axle suspension units, connected with the bogie frame by means of a pivot bearing. The axle suspension units incorporate one spring unit, consisting of a dual gas pressure accumulator. The gas pressure accumulator consists of a pressure reservoir, a flexible diaphragm and a hydraulic body with a non-return valve. Upon deflection of the axle suspension units, the displaced oil from the axle compensation cylinder is supplied to the gas pressure accumulator. The diaphragm and the nitrogen of the gas-pressure accumulator damp the hydraulic oil flow, thus enabling the compression and rebound of the axle suspension units.

No information has been given for the tractor wherefore leaf springs in front and air springs in rear are assumed. All wheels of the trailer have 8.25R15PR18 tyres and the tractor wheels are assumed to have 295/80R22.5.

2.2 Description of the Bridge

The considered bridge, see figure 2.3, is a part of the road Åsvej in the municipality of Roskilde on the island Zealand in Denmark. The bridge is considered for the project since measurements of the road irregularities exist from the stationing 15.872 km (record no. 7722) to the stationing 15.672 km (record no. 9692) with 0.1 m between each record number., i.e. a road with a length of 200 m has been measured. In the present project these data have been analysed and a stochastic modelling of the surface irregularities is presented, see Nielsen et al. (1997). Elevation and cross-section details for the considered bridge are given in figures 2.3 and 2.4. The bridge super structure is a continuous deck over the supporting columns. The supports for the deck are pinned, with rollers at all but not at the columns. From figures 2.3 and 2.4 it is seen that the total length of the bridge deck is 31.280 m, the width is 12.3 m and the deck thickness is 0.75 m. The columns are approximately 4.3 m long with cross sectional dimensions 1.0 x 0.6 m.

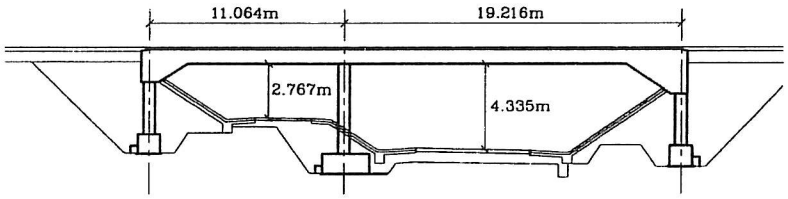

Figure 2.3 *Elevation details for the considered bridge*

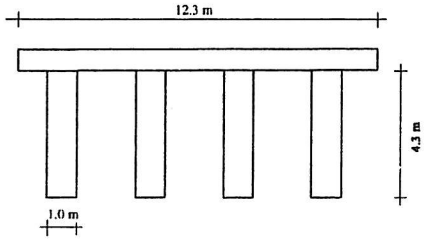

Figure 2.4 *Cross-section details for the considered bridge*

3. MODELLING OF VEHICLES

Based on the specification of the vehicles given in sections 2.1 and 2.2, respectively, the governing differential equation for the dynamic vehicle response will be given in the following.

3.1 Modelling of the Scania Heavy Lorry

From the dynamic analysis point of view, the Scania vehicle is composed of the body, suspension system and tyres. The vehicle body is assumed represented by a distributed mass subjected to rigid-body motions. Vertical displacements, pitching and roll rotations will be considered. Figure 3.1 shows the mathematical model of the vehicle and the degrees of freedom needed to describe its movement.

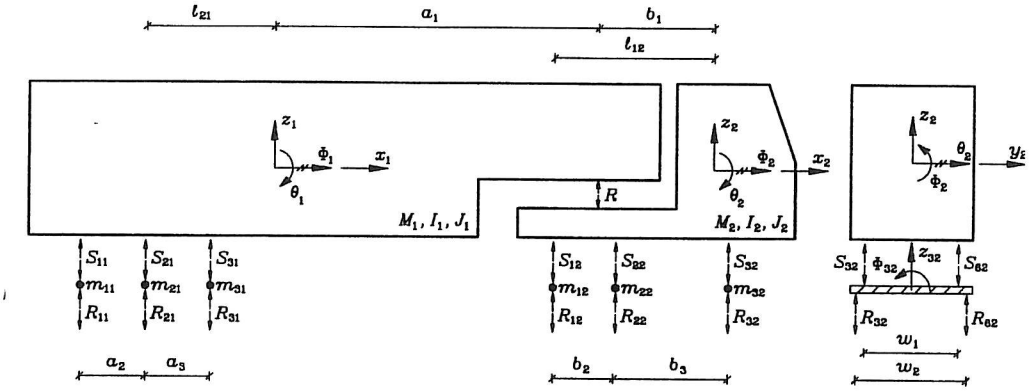

Figure 3.1 *Vehicle model and definition of degrees-of -freedom of the Scania vehicle.*

For the vehicle in figure 3.1 it is assumed that the two modules are linked together at a hinge, a so-called fifth wheel point, allowing rotations in all directions, so that only vertical forces are transmitted between the modules., i.e. the roll stiffness of the fifth wheel is neglected. The modules are assumed to be infinitely stiff with the coordinate axes (x_1,y_1,z_1) and (x_2,y_2,z_2) as principal axes of inertia. A local coordinate system is placed in the mass center of gravity of the modules with the three axes orientated in the vertical direction, the transverse direction and the longitudinal direction along the vehicle direction. The modules are free to move along the vertical direction and rotate about the two other axes. Hence, each module has three degrees of freedom, corresponding to the vertical displacements (heave) $z_1(t)$, $z_2(t)$, rotations about the transverse axis (pitch) $\theta_1(t), \theta_2(t)$, and rotations about the longitudinal axis (roll) $\phi_1(t)$, $\phi_2(t)$, respectively with sign defined in figure 3.1. These quantities are measured from the position of static equilibrium. I_1, I_2 signify the mass moments of inertia of rotation about the transverse axis and J_1, J_2 signify the mass moments of inertia of rotation about the longitudinal axis. M_1, M_2 are the masses of the modules. The modules are supported by spring forces $S_{i1}(t)$, $S_{i2}(t)$ acting between the modules and the axles modelling the suspension system of the vehicle. The sign of the spring forces when acting on the modules and the axles is shown on figure 3.1. The spring forces are acting symmetrical about the longitudinal axis with a distance w_1 in the transversal-direction. The abscissa, in the local coordinates centred at the mass centres, of the

springs attached to the axles are denoted l_{i1}, l_{i2}. Each axle is free to move in the vertical direction and to rotate around the longitudinal axis. Hence, each axle has 2 degrees of freedom, which are selected as the rotations $\phi_{i1}(t),\phi_{i2}(t)$ about the local centre of gravity in the longitudinal direction and the translations $z_{i1}(t)$, $z_{i2}(t)$ in the vertical direction. J_{i1}, J_{i2} and m_{i1}, m_{i2} denote the mass moments of inertia and the masses of the axles, respectively. The mass of the axles, wheels and brakes are concentrated under the suspension system and over a set of reaction forces $R_{i1}(t)$, $R_{i2}(t)$ between the axles and the road surface denoted with positive sign in the upward direction, when acting on the axles, and positive sign in the downward direction when acting on the road surface as shown in figure 3.1. The reaction forces are transmitted through wheels which act as secondary springs. The reaction forces are acting symmetrically about the longitudinal axis with a distance w_2 in the transverse direction. The longitudinal distance between the mass center of gravity and the reaction forces $R_{i1}(t)$, $R_{i2}(t)$ is assumed to be the same as the distances to the spring force $S_{i1}(t)$, $S_{i2}(t)$. As explained, the vehicle modules are linked together. For these modules an artificial degree of freedom $z_0(t)$ is introduced, specifying the vertical displacement of the coupling point. The reaction force between the modules is termed $R(t)$ which is considered positive when acting on the trailer module and in the upward direction. The distances to the coupling point from the mass centers of gravity for the two modules are denoted a_1 and b_1, respectively. The distances between the wheel at the trailer module are denoted a_2 and a_3 , respectively, and b_2 at the tractor module. Using the definitions given above the governing differential equations for the module responses can be written as follows when the distances l_{i1}, l_{i2}. are used with sign and the wheels are numbered according to figure 3.1. Linear behaviour of all elements and small angular displacements are assumed. Further, spring and reaction forces are assumed to remain parallel to the vertical axis and transmit only compression and tensile forces.

$$M_1\ddot{z}_1 - \sum_{i=1}^{6} S_{i1} - R = 0 \qquad (1)$$

$$M_2\ddot{z}_2 - \sum_{i=1}^{6} S_{i2} + R = 0 \qquad (2)$$

$$I_1\ddot{\theta}_1 + \sum_{i=1}^{6} S_{i1}l_{i1} + Ra_1 = 0 \qquad (3)$$

$$I_2\ddot{\theta}_2 + \sum_{i=1}^{6} S_{i2}l_{i2} + Rb_1 = 0 \tag{4}$$

$$J_1\ddot{\Phi}_1 - \sum_{i=1}^{6} S_{i1}w_{s,i1} = 0 \quad \begin{cases} w_{s,i1} = -\frac{1}{2}w_1 , & i = 1,2,3 \\ w_{s,i1} = \frac{1}{2}w_1 , & i = 4,5,6 \end{cases} \tag{5}$$

$$J_2\ddot{\Phi}_2 - \sum_{i=1}^{6} S_{i2}w_{s,i2} = 0 \quad \begin{cases} w_{s,i2} = -\frac{1}{2}w_1 , & i = 1,2,3 \\ w_{s,i2} = \frac{1}{2}w_1 , & i = 4,5,6 \end{cases} \tag{6}$$

$$m_{i1}\ddot{z}_{i1} + S_{i1} + S_{i+3,1} - R_{i1} - R_{i+3,1} = 0 , \; i = 1,2,3 \tag{7}$$

$$m_{i2}\ddot{z}_{i2} + S_{i2} + S_{i+2,2} - R_{i2} - R_{i+2,2} = 0 , \; i = 1,2,3 \tag{8}$$

$$J_{i1}\ddot{\Phi}_{i1} - \frac{1}{2}w_1(S_{i1} - S_{i+3,1}) + \frac{1}{2}w_2(R_{i1} - R_{i+3,1}) = 0 , \; i = 1,2,3 \tag{9}$$

$$J_{i2}\ddot{\Phi}_{i2} - \frac{1}{2}w_1(S_{i2} - S_{i+2,2}) + \frac{1}{2}w_2(R_{i2} - R_{i+2,1}) = 0 , \; i = 1,2,3 \tag{10}$$

By using the artificial degree of freedom $z_0(t)$ which specifies the vertical displacement of the coupling point the following relation between the two modules can be written

$$z_0(t) = z_1(t) - \theta_1(t)a_1 = z_2(t) + \theta_2(t)b_1 \tag{11}$$

which implies that $\theta_2(t)$ is given by

$$\theta_2(t) = \boldsymbol{a}z(t) , \; \boldsymbol{a} = \{1/b_1, -a_1/b_1, -1/b_1\} , \; z(t) = \{z_1(t), \theta_1(t), z_2(t)\}^T \tag{12}$$

By using (4) the reaction force between the modules $R(t)$ can be written

$$R(t) = -\frac{1}{b_1}\left(I_2 a\ddot{z} + \sum_{i=1}^{4} S_{i2} l_{i2} \right) \tag{13}$$

which can be used together with (1), (2) and (3), respectively, i.e. the number of degree of freedoms for the two modules can be reduced by one. By introducing a state vector for the Scania vehicle

$$z_s(t) = \{z_1, \theta_1, \phi_1, z_2, \phi_2, z_{11}, \phi_{11}, z_{21}, \phi_{21}, z_{31}, \phi_{31}, z_{12}, \phi_{12}, z_{22}, \phi_{22}, z_{32}, \phi_{32}\}^T \tag{14}$$

the governing response equations for the two modules can be written, see appendix A

$$\boldsymbol{M}_s \ddot{\boldsymbol{z}}_s + \boldsymbol{T}_s = \boldsymbol{0} \tag{15}$$

The spring forces $S_{i1}(t)$, $S_{i2}(t)$ and the reaction forces $R_{i1}(t)$, $R_{i2}(t)$ are modelled by the system shown in figure 3.2. This model is the most common description of vehicle suspension hysteresis characteristics used in vehicle simulation, but the accuracy of the model is often unsatisfactory, due to an overestimation of the response force, Kirkegaard et al. (1997). However, due to lack of information concerning the suspension system from the manufactures of the Scania and Goldhofer vehicles, it is chosen to use this model for the simulation model. The model for the spring forces consists of a linear spring with a spring constant $k_{s,ij}$ in parallel with a linear viscous damping element with a damping constant $c_{s,ij}$ and a constant Coulomb friction force $F_{s,ij}$. The model for the reaction forces modelling the tyres consists of a linear spring with a spring constant $k_{t,ij}$ in parallel with a linear viscous damping element with a damping constant $c_{t,ij}$.

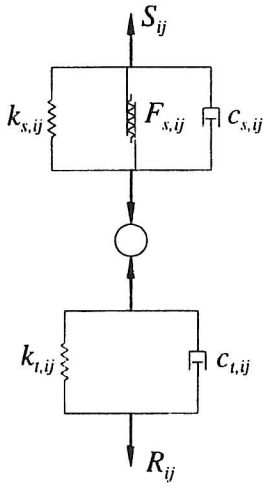

Figure 3.2 *Model of the spring forces and the reaction forces.*

The axial spring force in the suspension system for the two modules is written as follows, when the signs for w_{i1} and w_{i2} given in (5) and (6) are used

$$S_{i1} = -\left(k_{s,i1}z_{s,i1} + c_{s,i1}\dot{z}_{s,i1} + F_{s,i1}\frac{\dot{z}_{s,i1}}{|\dot{z}_{s,i1}|}\right) \tag{16}$$

$$S_{i2} = -\left(k_{s,i2}z_{s,i2} + c_{s,i2}\dot{z}_{s,i2} + F_{s,i2}\frac{\dot{z}_{s,i2}}{|\dot{z}_{s,i2}|}\right) \tag{17}$$

$$z_{s,i2} = z_2 - l_{i2}\theta_2 + \frac{1}{2}w_{s,i2}\phi_2 - z_{i2} - \frac{1}{2}w_{s,i2}\phi_{i2} \tag{18}$$

$$z_{s,i1} = z_1 - l_{i1}\theta_1 + \frac{1}{2}w_{s,i1}\phi_1 - z_{i1} - \frac{1}{2}w_{s,i1}\phi_{i1} \tag{19}$$

$z_{s,ij}$ is the relative displacement between the ith axle and the module. The axial dynamic reaction force of the ith wheel between the bridge and the vehicle is given as

$$R_{i1} = -\left(k_{t,i1}z_{t,i1} + c_{t,i1}\dot{z}_{t,i1} \right) \tag{20}$$

$$z_{t,i1} = (z_{i1} + \frac{1}{2}w_{t,i1}\phi_{i1} + u_{i1} - r_{i1}) \qquad \begin{cases} w_{t,i1} = -\frac{1}{2}w_2 , & i = 1,2,3 \\ w_{t,i1} = \frac{1}{2}w_2 , & i = 4,5,6 \end{cases} \tag{21}$$

$$R_{i2} = -\left(k_{t,i2}z_{t,i2} + c_{t,i2}\dot{z}_{t,i2} \right) \tag{22}$$

$$z_{t,i2} = (z_{i2} + \frac{1}{2}w_{t,i2}\phi_{i2} + u_{i2} - r_{i2}) \quad \begin{cases} w_{t,i2} = -\frac{1}{2}w_2 , & i = 1,2,3 \\ w_{t,i2} = \frac{1}{2}w_2 , & i = 4,5,6 \end{cases} \tag{23}$$

$z_{t,ij}$ is the displacement of the axle relative to the mean level of the surface irregularities. $u_{ij}(x,t)$ and $r_{ij}(x,t)$ are the vertical bridge displacement (positive downwards) and the road surface irregularity i.e. bump and road roughness (positive upwards) at the position of the reaction forces R_{ij}. It is assumed that the vehicle never loses contact with the bridge. The location $\mathbf{x}$ of the contact point at the time t is composed of coordinate axes x_1 and x_2 which are the longitudinal and the transverse direction of the bridge, respectively.

3.1.1 Physical Parameters for the Scania Vehicle Model

The physical parameters for the Scania are listed in the following tables. The geometric and inertia properties are based on information from Ole M. Jørgensen, Scania Denmark and Tor Langhed, Scania Sweden.

Geometric Properties	
a_1 (m)	5.61
a_2 (m)	1.56
a_3 (m)	1.56
l_{11} (m)	-4.76
l_{21} (m)	-3.20
l_{31} (m)	-1.64
b_1 (m)	1.80
b_2 (m)	3.70
l_{12} (m)	-2.45
l_{22} (m)	1.25
w_1 (m)	1.60 (front axle)
w_1 (m)	0.77 (rear axle)
w_1 (m)	1.60 (trailer)

w_2 (m)	1.80 (front axle)
w_2 (m)	1.80 (rear axle)
w_2 (m)	1.80 (trailer)

Table 3.1 *Geometry for the Scania.*

Inertia Properties	
I_1 (kgm^2)	20488
I_2 (kgm^2)	4604
J_1 (kgm^2)	425520
J_2 (kgm^2)	41111
J_{i1} (kgm^2)	600
J_{i2} (kgm^2)	600 (front axle)
J_{i2} (kgm^2)	1000 (rear axle)
M_1 (kg)	39400
M_2 (kg)	4500
m_{i1} (kg)	700
m_{i2} (kg)	700 (front axle)
m_{i2} (kg)	1300 (rear axle)

Table 3.2 *Inertia properties for the Scania.*

It is assumed that the 6 spring forces for the trailer are identical. Similarly, the 6 reaction forces are identically modelled. The parameters for the trailer are chosen equal to the parameters for the front suspension of the tractor. The rear suspension system has air springs. Parameters for the leaf springs were given from Scania in Sweden. Other parameters are based upon values given in the literature.

Suspension Properties		
	Tractor	Trailer
$k_{s,ij}$ (10^3 N/m).	1800 (front axle)	1800
$k_{s,ij}$ (10^3 N/m)	300 (rear axle)	-
$c_{s,ij}$ (Ns/m)	5000	5000
$F_{s,ij}$ (N)(pull)	4000	4000

$F_{s,ij}$ (N)(comp)	2000	2000
$k_{t,ij}$ (10^3 N/m)	1000 (front axle)	-
$k_{t,ij}$ (10^3 N/m)	2000	2000
$c_{t,ij}$ (Ns/m)	3000	3000

Table 3.3 *Suspension properties for the Scania.*

3.2 Modelling of the Goldhofer SKPH 8 Special Transportation

The Goldhofer vehicle is modelled using the same assumptions as stated for the Scania vehicle, i.e. vertical displacements, pitching and roll rotations will be considered. Figure 3.3 shows the mathematical model for the Goldhofer vehicle and the degrees of freedom needed to describe its movement.

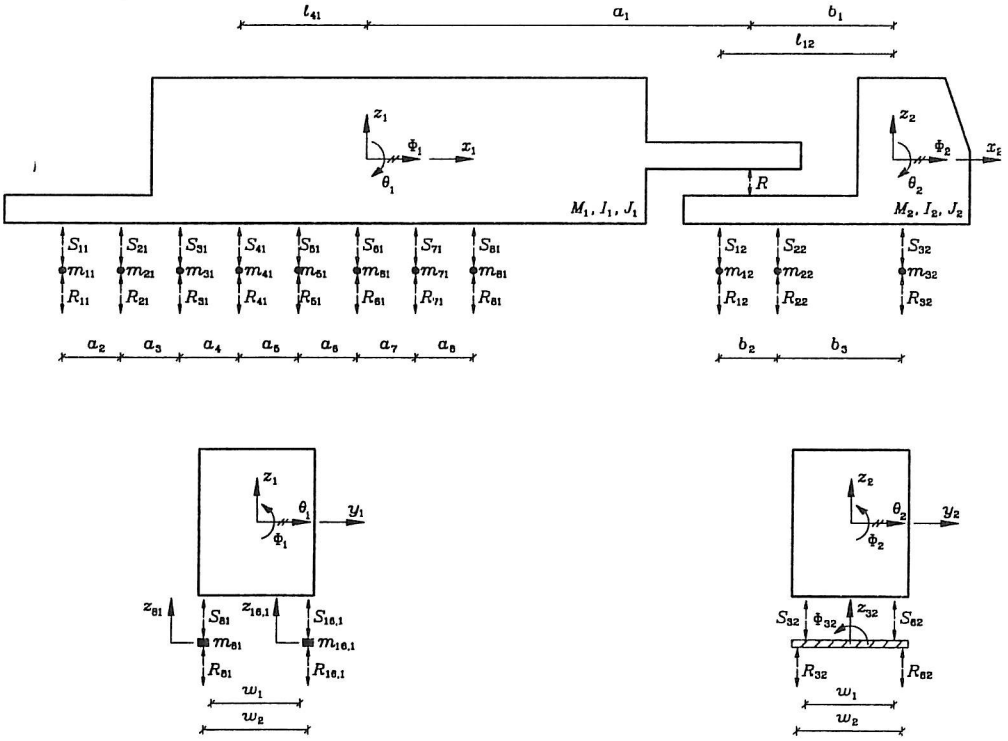

Figure 3.3 *Vehicle model and definition of degrees of freedom for the Goldhofer SKPH 8 Special Transportation*

For the vehicle in figure 3.3 it is assumed that the two modules are linked together at a hinge, a so-called fifth wheel point, allowing rotations in all directions, so that only vertical and horisontal forces are transmitted between the modules., i.e. that the roll stiffness of the fifth wheel is neglected. The modules are assumed to be infinitely stiff with the coordinate axes (x_1,y_1,z_1) and (x_2,y_2,z_2) as principal axes of inertia. A local coordinate system is placed in the mass center of gravity of the modules, with the three axes orientated in the vertical direction, the transverse and the longitudinal direction along

the vehicle direction. The modules are free to move along the vertical direction and rotate about the two other axes. Hence each modul has three degrees of freedom, corresponding to the vertical displacements (heave) $z_1(t)$, $z_2(t)$, rotations about the transverse axis (pitch) $\theta_1(t), \theta_2(t)$, and rotations about the longitudinal axis (roll), $\phi_1(t)$, $\phi_2(t)$, respectively, with sign defined in figure 3.3. These quantities are measured from the position of static equilibrium. I_1, I_2 signify the mass moments of inertia of rotation about the transverse axis and J_1, J_2 signify the mass moments of inertia of rotation about the longitudinal axis. M_1, M_2 are the masses of the modules. The modules are supported by spring forces $S_{i1}(t)$, $S_{i2}(t)$ acting between the modules and the axles modelling the suspension system of the vehicle. The sign of the spring forces when acting on the modules and the axles is shown on figure 3.3. The spring forces are acting symmetrically about the longitudinal axis at a distance w_1 in the transverse-direction. The abscissa, in the local coordinates centered at the mass centres, of the springs attached to the axles are denoted l_{i1}, l_{i2}. Each tractor axle is free to move in the vertical direction and to rotate around the longitudinal axis. Hence, each axle has 2 degrees of freedom, which are selected as the rotation $\phi_{i2}(t)$ about the local centre of gravity in the longitudinal direction and the translation $z_{i2}(t)$ in the vertical direction. J_{i2} and m_{i2} denote the mass moment of inertia and the mass of the axles, respectively. From figure 3.3 it is seen that each trailer wheel has its own axle which is modelled by one degree of freedom, i.e. the translations $z_{i1}(t)$ in the vertical direction. m_{i1} denotes the mass of the trailer axle. The mass of the axles, wheels and brakes for the whole Goldhofer vehicle are assumed concentrated under the suspension system and over a set of reaction forces $R_{i1}(t)$, $R_{i2}(t)$ between the axles and the road surface denoted with positive sign in the upward direction, when acting on the axles, and positive sign in the downward direction when acting on the road surface as shown in figure 3.3. The reaction forces are transmitted through wheels which act as secondary springs. The reaction forces are acting symmetrically about the longitudinal axis at a distance w_2 in the transverse direction. The longitudinal distance between the mass center of gravity and the reaction forces $R_{i1}(t)$, $R_{i2}(t)$ is assumed to be the same as the distances to the spring force $S_{i1}(t)$, $S_{i2}(t)$. As explained, the vehicle modules are linked together. For these modules an artificial degree of freedom $z_0(t)$ is introduced, specifying the vertical displacement of the coupling point. The reaction force between the modules is termed $R(t)$ which is considered positive when acting on the trailer module and in the upward direction. The distances to the coupling point from the mass centers of gravity for the two modules are denoted a_1 and b_1, respectively. The distances between the wheel at the trailer module are denoted a_2, a_3, a_4 , a_5 , a_6 , a_7 and a_8, respectively, and b_2 and b_3 at the tractor module. Using the definitions given above the governing differential equations for the module responses can be written as follows when the distances l_{i1}, l_{i2} are used with sign and the wheels are numbered according to figure 3.3. Linear behaviour of all elements and small angular displacements are assumed. Further, the spring and reaction forces are assumed to remain parallel to the vertical axis and transmit only compression and tensile forces.

$$M_1\ddot{z}_1 - \sum_{i=1}^{16} S_{i1} - R = 0 \tag{24}$$

$$M_2\ddot{z}_2 - \sum_{i=1}^{6} S_{i2} + R = 0 \tag{25}$$

$$I_1\ddot{\theta}_1 + \sum_{i=1}^{16} S_{i1}l_{i1} + Ra_1 = 0 \tag{26}$$

$$I_2\ddot{\theta}_2 + \sum_{i=1}^{6} S_{i2}l_{i2} + Rb_1 = 0 \tag{27}$$

$$J_1\ddot{\Phi}_1 - \sum_{i=1}^{16} S_{i1}w_{s,i1} = 0 \quad \begin{cases} w_{s,i1} = -\frac{1}{2}w_1 , & i = 1,..,8 \\ w_{s,i1} = \frac{1}{2}w_1 , & i = 9,..,16 \end{cases} \tag{28}$$

$$J_2\ddot{\Phi}_2 - \sum_{i=1}^{6} S_{i2}w_{s,i2} = 0 \quad \begin{cases} w_{s,i2} = -\frac{1}{2}w_1 , & i = 1,2,3 \\ w_{s,i2} = \frac{1}{2}w_1 , & i = 4,5,6 \end{cases} \tag{29}$$

$$m_{i1}\ddot{z}_{i1} + S_{i1} - R_{i1} = 0 , \; i = 1,2,..,16 \tag{30}$$

$$m_{i2}\ddot{z}_{i2} + S_{i2} + S_{i+3,2} - R_{i2} - R_{i+3,2} = 0 , \; i = 1,2,3 \tag{31}$$

$$J_{i2}\ddot{\Phi}_{i2} - \frac{1}{2}w_1(S_{i2} - S_{i+3,2}) + \frac{1}{2}w_2(R_{i2} - R_{i+3,1}) = 0 , \; i = 1,2,3 \tag{32}$$

An artificial degree of freedom $z_0(t)$ which specifies the vertical displacement of the coupling point is introduced. The relation (27) implies that the reaction force $R(t)$ between the two modules can be written using (12)

$$R(t) = -\frac{1}{b_1}\left(I_2 a\ddot{z} + \sum_{i=1}^{6} S_{i2} l_{i2} \right) \tag{33}$$

which can be used together with (24), (25) and (26), respectively, i.e. the number of degree of freedom for the two modules can be reduced by one. By introducing a state vector

$$\begin{aligned} z_s(t) = \{ & z_1, \theta_1, \phi_1, z_2, \phi_2, z_{11}, z_{21}, z_{31}, z_{41}, z_{51}, z_{61}, z_{71}, z_{81}, z_{91}, z_{101}, \\ & z_{111}, z_{121}, z_{131}, z_{141}, z_{151}, z_{161}, z_{12}, \phi_{12}, z_{22}, \phi_{22}, z_{22}, \phi_{32} \}^T \end{aligned} \tag{34}$$

the governing response equations for the two modules can be written, see appendix B

$$M_g \ddot{z}_g + T_g = 0 \tag{35}$$

The spring forces $S_{i1}(t)$, $S_{i2}(t)$ and the reaction forces $R_{i1}(t)$, $R_{i2}(t)$ are modelled by the system used for the Scania vehicle shown in figure 3.2, i.e. the axial spring force in the suspension system for the two modules can be written

$$S_{i1} = -\left(k_{s,i1} z_{s,i1} + c_{si} \dot{z}_{s,i1} + F_{s,i1} \frac{\dot{z}_{s,i1}}{|\dot{z}_{s,i1}|} \right) \tag{36}$$

$$S_{i2} = -\left(k_{s,i2} z_{s,i2} + c_{s,i2} \dot{z}_{s,i2} + F_{s,i2} \frac{\dot{z}_{s,i2}}{|\dot{z}_{s,i2}|} \right) \tag{37}$$

$$z_{s,i1} = z_1 - l_{i1}\theta_1 + \frac{1}{2} w_{s,i1} \phi_1 - z_{i1} \tag{38}$$

$$z_{s,i2} = z_2 - l_{i2}\theta_2 + \frac{1}{2} w_{s,i2} \phi_2 - z_{i2} - \frac{1}{2} w_{s,i2} \phi_{i2} \tag{39}$$

$z_{s,ij}$ is the relative displacement between the ith axle and the module. The axial dynamic reaction force of the ith wheel between the bridge and the vehicle is given as

$$R_{i1} = -\left(k_{t,i1} z_{t,i1} + c_{t,i1} \dot{z}_{t,i1} \right) \tag{40}$$

$$z_{t,i1} = z_{i1} + u_{i1} - r_{i1} \tag{41}$$

$$R_{i2} = -\left(k_{t,i2} z_{t,i2} + c_{t,i2} \dot{z}_{t,i2} \right) \tag{42}$$

$$z_{t,i2} = z_{i2} + \frac{1}{2} w_{t,i2} \phi_{i2} + u_{i2} - r_{i2} \qquad \begin{cases} w_{t,i2} = -\frac{1}{2} w_1 , & i = 1,2,3 \\ w_{t,i2} = \frac{1}{2} w_2 , & i = 4,5,6 \end{cases} \tag{43}$$

$z_{t,ij}$ is the displacement of the axle relative to the mean level of the surface irregularities. $u_{ij}(x,t)$ and $r_{ij}(x,t)$ are the vertical bridge displacement (positive downwards) and the road surface irregularity i.e. bump and road roughness (positive upwards) at the position of the reaction forces R_{ij}. It is assumed that the vehicle never loses contact with the bridge. The location x of the contact point at the time t is composed of coordinate axes x_1 and x_2 which are the longitudinal and the transverse direction of the bridge, respectively.

3.2.1 Physical Parameters for the Goldhofer Vehicle Model

The physical parameters for the Goldhofer SKPH 8 are listed in the following tables. Due to lack of information from Goldhofer, it is chosen to use the parameters for a Scania tractor for the Goldhofer tractor. These data were available from Scania. The stiffness data for the trailer are based on information from BPW, Germany, who is the manufactor of the axles for the trailer.

Geometric Properties	
a_1 (m)	9.45
a_2 (m)	1.36
a_3 (m)	1.36
a_4 (m)	1.36
a_5 (m)	1.36
a_6 (m)	1.36
a_7 (m)	1.36
a_8 (m)	1.36
l_{11} (m)	-6.85

l_{21} (m)	-5.49
l_{31} (m)	-4.13
l_{41} (m)	-2.77
l_{51} (m)	-1.41
l_{61} (m)	-0.5
l_{71} (m)	1.31
l_{81} (m)	2.67
b_1 (m)	1.99
b_2 (m)	1.36
b_3 (m)	2.75
l_{12} (m)	-2.71
l_{22} (m)	-1.36
l_{32} (m)	1.39
w_1 (m)	1.60 (front axle)
w_1 (m)	0.77 (rear axle)
w_1 (m)	1.80 (trailer)
w_2 (m)	1.80 (front axle)
w_2 (m)	1.80 (rear axle)
w_2 (m)	1.80 (trailer)

Table 3.4 *Geometry for the Goldhofer SKPH 8.*

Inertia Properties	
I_1 (kgm^2)	484034
I_2 (kgm^2)	5320
J_1 (kgm^2)	1005307
J_2 (kgm^2)	47506
J_{i2} (kgm^2)	600 (front axle)
J_{i2} (kgm^2)	1000 (rear axle)

M_1 (kg)	93084
M_2 (kg)	5200
m_{i1} (kg)	276
m_{i2} (kg)	700 (front axle)
m_{i2} (kg)	1300 (rear axle)

Table 3.5 *Inertia properties for the Goldhofer SKPH 8.*

It is assumed that the spring forces for the trailer are identical, i.e. the parameters $k_{s,ij}$, $c_{s,ij}$ and $F_{s,ij}$ are identical. Similarly, the reaction forces are identically modelled.

Suspension Properties		
	Tractor	Trailer
$k_{s,ij}$ (10^3 N/m)	1800 (front axle)	1800
$k_{s,ij}$ (10^3 N/m)	300 (rear axle)	-
$c_{s,ij}$ (Ns/m)	5000	5000
$F_{s,ij}$ (N)(pull)	4000	4000
$F_{s,ij}$ (N)(comp)	2000	2000
$k_{t,ij}$ (10^3 N/m)	1000 (front axle)	-
$k_{t,ij}$ (10^3 N/m)	2000	2000
$c_{t,ij}$ (Ns/m)	3000	3000

Table 3.6 *Suspension properties for the Goldhofer SKPH 8.*

4. MODELLING OF BRIDGE RESPONSE TO VEHICLE LOADS

Based on the specification of the bridge given in section 2.2 the governing differential equation for the dynamic bridge response will be given in the following. The dynamic response of the bridge is rather insignificant for the present short-span bridges. For this reason a truncated normal mode expansion is used, which preserves the basic quasi-static response of the bridge and includes the dynamic response of the few lowest eigenmodes.

4.1 Modelling of the Bridge

The considered bridge constitutes the part l_0 of the road with the length L as shown in figure 4.1. The bridge is a two span typical Danish highway bridge with supporting columns as described in section 2.2.

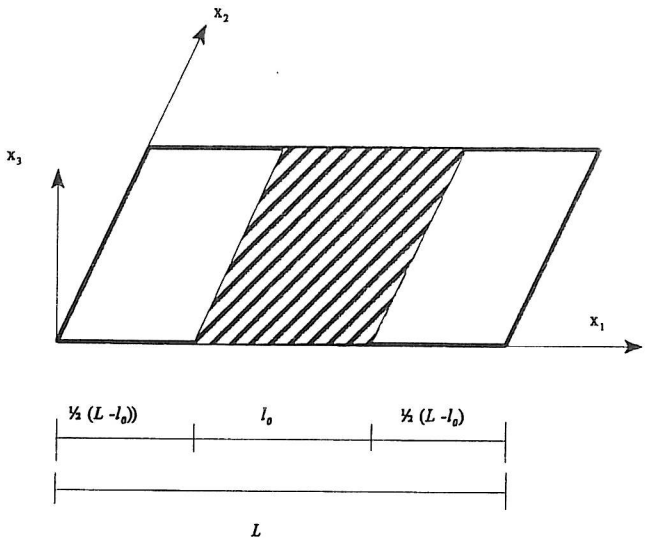

Figure 4.1 *Definition of the bridge part (hatched) of the road*

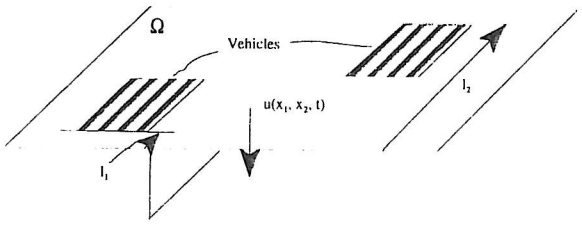

Figure 4.2 *Idealized description of bridge*

Figure 4.2 shows an idealized model of the linear elastic bridge with two vehicles. The vehicles move in the x_1 -direction in the distances l_1 and l_2 from the edge of the bridge corresponding to the x_2 -axis. The stiffness and the mass are assumed isotropic and homogeneous. Further, viscous damping is assumed. Using modal decomposition to the order N the vertical deflection $u(x_1, x_2, t)$ can be written

$$u(x_1,x_2,t) = \sum_{j=i}^{N} q_j(t)\ \Phi^{(j)}(x_1,x_2) + \sum_{i=1}^{N_w} \int_{\Omega} I_u\left(x_1,x_2;x_{1,i}(t),x_{2,i}(t)\right)\delta(x_1 - x_{1,i}(t))\delta(x_2 - x_{2,i}(t))F_i(x_1(t),x_2(t),t)J_i(t)dx_1dx_2 \tag{44}$$

where

$$I_u(x_1,x_2;y_1,y_2) = I(x_1,x_2;y_1,y_2) - \sum_{j=1}^{N} \frac{1}{\omega_j^2 M_j}\Phi^{(j)}(x_1,x_2)\Phi^{(j)}(y_1,y_2) \tag{45}$$

N_w is the number of wheels, F_i(t) is the ith wheel load from R_{ij} , J_i(t) is an indicator function equal 1 when the ith wheel is on the bridge and $x_{1,i}$(t), $x_{2,i}$(t) signifies its position at the time t. $I(x_1,x_2;y_1,y_2)$ is the statical influence function respresenting the displacement at (x_1 x_2) from a unit static force at (y_1 y_2). (45) is derived based on the eigenmode expansion of $I(x_1,x_2;y_1,y_2)$ (Mercer's theorem), see Nielsen (1993). $\Phi^{(j)}(x_1,x_2)$ is the jth mode shape, ω_j is the jth undamped circular eigenfreqeuncy and M_j is the jth modal mass. The modal coordinates $q_j(t)$ are assumed to be decoupled as given by the following differential equantions

$$\ddot{q}_j + 2\zeta\omega_j\dot{q}_j + \omega_j^2 q_j = \frac{1}{M_j}\sum_{i=1}^{N_w}\int_{\Omega}\Phi^{(j)}(x_1,x_2)\delta(x_1 - x_{1,i}(t))\delta(x_2 - x_{2,i}(t))F_i(x_1(t),x_2(t),t)J_i(t)dx_1dx_2 \tag{46}$$

By introducing a state vector for the model quantities

$$z_b(t) = \{q_1,q_2,\ldots,q_N\}^T \tag{47}$$

the governing response equations for the bridge can be written

$$\ddot{z}_b + T_b = 0 \tag{48}$$

where the jth elements of T_b are given by

$$T_b^j = 2\zeta\omega_j\dot{q}_j + \omega_j^2 q_j - \frac{1}{M_j}\sum_{i=1}^{N_w}\int_{\Omega}\Phi^{(j)}(x_1,x_2)\delta(x_1 - x_{1,i}(t))\delta(x_2 - x_{2,i}(t))F_i(t)J_i(t)dx_1dx_2 \tag{49}$$

5. COMPUTATIONAL PROCEDURES

Based on the modelling of the vehicles and the bridge a MATLAB program has been developed. The following sections give an outline of the developed program.

5.1 The MATLAB program

This program makes it possible to simulate the bridge response where the speed of the vehicles, their mutual position at the opposite entrance of the bridge, the surface irregularities, the height and wavelength of the bumps, and the parameters of the vehicles can be varied. The following crossing scenarios can be considered

- one Scania vehicle at a given velocity moves across the bridge along a given straight path

- one Goldhofer vehicle at a given velocity moves across the bridge along a given straight path

- two Scania vehicles at given velocities move across the bridge along given straight paths, both in the same direction or one in each direction

- two Goldhofer vehicles at given velocities move across the bridge along given straight paths, both in the same direction or one in either direction

- one Scania and one Goldhofer vehicle at given velocities move across the bridge along given straight paths, both in the same direction or one in either direction

The the moving paths for the vehicles can be chosen different for each crossing scenario. Further, the program allows simulation of

- a given number of moving forces, moving masses or moving sprung masses which move across a bridge along given straight paths

- the bridge response for a given bridge structure when the mode shapes have been estimated by FEM

The program has been developed for use with PC-MATLAB 4.2

5.2 Numerical Solution Methods

Based on the equations (15), (35) and (48) the following set of coupled first order differential equations can be obtained .

$$\frac{d}{dt}\begin{bmatrix} z_b \\ z_s \\ z_g \\ \dot{z}_b \\ \dot{z}_s \\ \dot{z}_g \end{bmatrix} = \begin{bmatrix} \dot{z}_b \\ \dot{z}_s \\ \dot{z}_g \\ -T_b \\ -M_s^{-1}T_s \\ -M_g^{-1}T_g \end{bmatrix} \tag{50}$$

In order to solve (50) the bridge displacement response has to be estimated for each time step using the modal decomposition (44) which is implemented using quasi-static correction. This implies that only a limited number of modes for the full problem shall be determined, and the effect of the remaining - undetermined - modes is included by an approximated static analysis. The basis of this method is that a large number of high frequency modes essentially respond in a quasi-static way and therefore only modes which give rise to dynamic amplification are taken into account in the reduced modal decomposition for the structural systems, i.e. the state vector z_b can be reduced to only some few quantities N.

By using (44) the bending moment $M(x_1,x_2,t)$ and shear force $Q(x_1,x_2,t)$ at a point $(x_1,x_2,)$ typically located over the intermediate supports and the midspan for the moment and at the entrance to the bridge for the shear force are estimated as

$$M(x_1,x_2,t) = \sum_{j=i}^{N} q_j(t)\ M^{(j)}(x_1,x_2) + \sum_{i=1}^{N_w} \int_{\Omega} I_M\left(x_1,x_2;x_{1,i}(t),x_{2,i}(t)\right)\delta(x_1 - x_{1,i}(t))\delta(x_2 - x_{2,i}(t))F_i(x_1(t),x_2(t),t)J_i(t)dx_1dx_2 \tag{51}$$

$$Q(x_1,x_2,t) = \sum_{j=i}^{N} q_j(t)\ Q^{(j)}(x_1,x_2) + \sum_{i=1}^{N_w} \int_{\Omega} I_Q\left(x_1,x_2;x_{1,i}(t),x_{2,i}(t)\right)\delta(x_1 - x_{1,i}(t))\delta(x_2 - x_{2,i}(t))F_i(x_1(t),x_2(t),t)J_i(t)dx_1dx_2 \tag{52}$$

where the influence functions $I_M(x_1,x_2;x_1(t),x_2(t))$ and $I_Q(x_1,x_2;x_1(t),x_2(t))$ are estimated as described for the influence function for the displacement (45). $M^{(j)}(x_1,x_2)$ and $Q^{(j)}(x_1,x_2)$ are the bending moment and the shear force when the bridge deck is deformed according to the jth mode shape $\Phi^{(j)}(x_1,x_2)$. However, these functions were not available from the FEM solution. Therefore, the bending moment $M_i^j = M^j(x_1,x_2)$ at point i at position (x_1,x_2) has been estimated as

$$M_i^j = \sum_{k=1}^{N_n} M_i^0 \Phi_k^j \omega_j^2 m_k \tag{53}$$

where Φ_k^j is the value of the jth mode shape at a node k with the nodal mass m_k. The mode shape is assumed to be discretized into N_n nodes. M_i^0 is a static influence value for a unit force. The shear force $Q_i^j = Q^j(x_1,x_2)$ at point i at position (x_1,x_2) has been estimated as

$$Q_i^j = \sum_{k=1}^{N_n} Q_i^0 \Phi_k^j \omega_j^2 m_k \tag{54}$$

where Q_i^0 is a static influence value for a unit force.

The surface roughness profile has been implemented by three different approaches as

- a sum of series of sinusoidal waves generated with random phase angles with uniform distribution in the interval $\{0;2\pi\}$. The amplitudes of the waves are related to a Power Spectral Density function.

- the measured road surface profile, see Nielsen et al. (1997).

- simulated road surface profiles given by the model proposed in Nielsen et al. (1997)

In order to model bumps at the entrance to the bridge half a sine function $r(x)$ given as

$$r(x_1) = \alpha_0[H(x_1-s_1)-H(x_1-s_2)]\sin\frac{\pi(s_2-x_1)}{s_2-s_1} \tag{55}$$

is used where α_0 characterizes the amplitude of the local irregularity while s_1 and s_2 are the abscissas of the points and H(•) is the unit step function. Due to the piecewise differentiability of the irregularity function (55), the domain of the irregularity function with respect to x_1 is divided into three intervals; $x_1 \le s_1$, $s_1 < x_1 < s_2$, $x_1 \ge s_2$ .The derivative within $s_1 < x_1 < s_2$ can be expressed as

$$\dot{r}(x_1) = -\alpha_0[H(x_1-s_1)-H(x_1-s_2)]\frac{\pi(s_2-x_1)}{s_2-s_1}\cos\frac{\pi(s_2-x_1)}{s_2-s_1} \tag{56}$$

It should be noted that in order to avoid mathematical difficulties in the numerical implementation it is ensured that the vehicle position and discontinuities in the surface irregularity function at $x_1 = s_1$ and $x_1 = s_2$ do not coincide.

5.3 FEM of the Bridge

The mode shape information used as input to the MATLAB program was obtained by modelling the bridge using the finite-element program STAAD-111, STAAD-111 (1993), assuming that the bridge

can be modelled as a linear model based on a finite number of modes. STAAD-111 is equipped with a state-of-the-art plate finite element formulation. This includes plane stress, plate bending, out of plane shear and flat shell triangular (three nodes) or quadrilateral (four node) elements. Variable thicknesses at different nodes are allowed. The bridge deck is modelled by isotropic plate elements, see figure 5.1, where a complete quadratic stress distribution is assumed, see STAAD-lll (1993). 45 and 8 elements have been used in the longitudinal and transverse direction, respectively. Each column has been modelled by 5 beam elements assumed to have fixed supports. The connections between the columns and the bridge deck have also been modelled as fixed. The supports at the ends of the bridges are modelled as pinned with rollers.

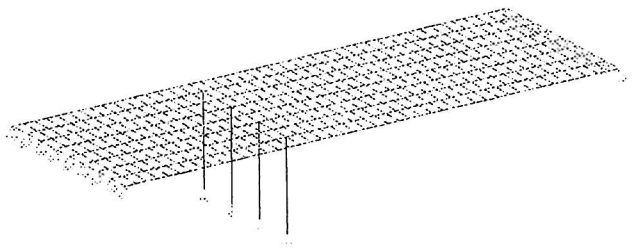

Figure 5.1 *Finite element model of the bridge.*

The reinforced concrete is considered as an isotropic material with the following properties: Young's modulus = 28000 MPa, Poisson's ratios = 0.3 and mass density 2800 kg/m^3. Cross-sectional quantities were calculated by the FEM program. The first 20 mode shapes are presented in appendix C. Table 5.1 gives the natural frequencies for the first 20 modes. Based on these values it is decided to take the first three modes into consideration in the calculation of the responses, since the dynamic wheel load is assumed to be in the range 0-10 Hz, see Kirkegaard et al. (1997).

Mode	1	2	3	4	5	6	7	8	9	10
Hz	3.43	6.75	10.18	12.41	15.03	15.79	17.70	24.82	25.63	26.89
Mode	11	12	13	14	15	16	17	18	19	10
Hz	31.38	34.81	38.09	39.67	41.04	42.96	45.25	47.34	51.91	53.42

Table 5.1 *First 20 natural frequencies for the bridge.*

6. ACKNOWLEDGEMENTS

The present research was partially supported by The Danish Technical Research Council within the project: "Dynamics of Structures", and "Dynamic Amplification Factor of Vehicle Loads for Reinforcement Projects on Small Highway Bridges". Further, Ole M. Jørgensen and Tor Langhed from Scania Denmark and Scania Sweden, respectively are acknowledged for kind release of information concerning the Scania vehicle.

7. REFERENCES

Nielsen, S.R.K., Kirkegaard, P.H. & Enevoldsen, I. *Heavy Vehicles on Minor Highway Bridges - Stochastic Modelling of Surface Irregularities.* Structural Reliability Theory Paper, No. 170, Department of Building Technology and Structural Engineering, Aalborg University, ISSN1395-7953R9720, 1997.

Kirkegaard, P.H., Nielsen, S.R.K. & Enevoldsen, I. *Heavy Vehicles on Minor Highway Bridges - A Literature Review.* Structural Reliability Theory Paper, No. 169, Department of Building Technology and Structural Engineering, Aalborg University, ISSN1395-4953R9719, 1997.

STAAD-111 - *Structural Analysis and Design Software*, Revision 21.0w, 1995.

Nielsen, S.R.K. *Linear Vibration Theory, Vol. 1.* (In Danish). Aalborg Technical University Press, ISSN0902-8005U9308, 1993.

Chompooming, K. & Yener, M. *The Influence of Roadway Surface Irregularities and Vehicle Deceleration on Bridge Dynamics using the Method of Lines.* Journal of Sound and Vibration,

Vejdirektoratet - *Beregningsregler for Eksisterende Broers Bæreevne.* April 1996.

APPENDIX A : Elements of M_s and T_s

$$M_s^{1,1} = M_1 + \frac{1}{b_1^2} I_2$$

$$M_s^{1,2} = -\frac{a_1}{b_1^2} I_2$$

$$M_s^{1,4} = -\frac{1}{b_1^2} I_2$$

$$M_s^{2,1} = -\frac{a_1}{b_1^2} I_2$$

$$M_s^{2,2} = I_1 + \frac{a_1^2}{b_1^2} I_2$$

$$M_s^{2,4} = \frac{a_1}{b_1^2} I_2$$

$$M_s^{3,3} = J_1$$

$$M_s^{4,1} = -\frac{1}{b_1} I_2$$

$$M_s^{4,2} = \frac{a_1}{b_1} I_2$$

$$M_s^{4,4} = M_2 + \frac{1}{b_1} I_2$$

$$M_s^{5,5} = J_2$$

$$M_s^{6,6} = m_{11}$$

$$M_s^{7,7} = J_{11}$$

$$M_s^{8,8} = m_{21}$$

$$M_s^{9,9} = J_{21}$$

$$M_s^{10,10} = m_{31}$$

$$M_s^{11,11} = J_{31}$$

$$M_s^{12,12} = m_{12}$$

$$M_s^{13,13} = J_{12}$$

$$M_s^{14,14} = m_{22}$$

$$M_s^{15,15} = J_{22}$$

$$M_s^{16,16} = m_{32}$$

$$M_s^{17,17} = J_{32}$$

All other elements in M_s are zero.

$$T_s^1 = -\sum_{i=1}^{6} S_{i1}$$

$$T_s^2 = \sum_{i=1}^{6} S_{i1} l_{i1}$$

$$T_s^3 = -\sum_{i=1}^{6} S_{i1} w_{i1}$$

$$T_s^4 = -\sum_{i=1}^{4} S_{i2}$$

$$T_s^5 = -\sum_{i=1}^{4} S_{i2} w_{i2}$$

$$T_s^6 = S_{11} + S_{41} - R_{11} - R_{41}$$

$$T_s^7 = -\frac{1}{2} w_1 (S_{11} - S_{41}) + \frac{1}{2} w_2 (R_{11} - R_{41})$$

$$T_s^8 = S_{21} + S_{51} - R_{21} - R_{51}$$

$$T_s^9 = -\frac{1}{2} w_1 (S_{21} - S_{51}) + \frac{1}{2} w_2 (R_{21} - R_{51})$$

$$T_s^{10} = S_{31} + S_{61} - R_{31} - R_{61}$$

$$T_s^{11} = -\frac{1}{2} w_1 (S_{31} - S_{61}) + \frac{1}{2} w_2 (R_{31} - R_{61})$$

$$T_s^{12} = S_{12} + S_{32} - R_{12} - R_{32}$$

$$T_s^{13} = -\frac{1}{2} w_1 (S_{12} - S_{32}) + \frac{1}{2} w_2 (R_{12} - R_{32})$$

$$T_s^{14} = S_{22} + S_{42} - R_{22} - R_{42}$$

$$T_s^{15} = -\frac{1}{2} w_1 (S_{22} - S_{42}) + \frac{1}{2} w_2 (R_{22} - R_{42})$$

$$T_s^{16} = S_{32} + S_{62} - R_{32} - R_{62}$$

$$T_s^{17} = -\frac{1}{2} w_1 (S_{32} - S_{62}) + \frac{1}{2} w_2 (R_{32} - R_{62})$$

All other elements in T_s are zero.

APPENDIX B : Elements of M_g and T_g

$$M_g^{1,1} = M_1 + \frac{1}{b_1^2} I_2$$

$$M_g^{1,2} = -\frac{a_1}{b_1^2} I_2$$

$$M_g^{1,4} = -\frac{1}{b_1^2} I_2$$

$$M_g^{2,1} = -\frac{a_1}{b_1^2} I_2$$

$$M_g^{2,2} = I_1 + \frac{a_1^2}{b_1^2} I_2$$

$$M_g^{2,4} = \frac{a_1}{b_1^2} I_2$$

$$M_g^{3,3} = J_1$$

$$M_g^{4,1} = -\frac{1}{b_1^2} I_2$$

$$M_g^{4,2} = \frac{a_1}{b_1^2} I_2$$

$$M_g^{4,4} = M_2 + \frac{1}{b_1^2} I_2$$

$$M_g^{5,5} = J_2$$

$$M_g^{6,6} = m_{11}$$

$$M_g^{7,7} = m_{21}$$

$$M_g^{8,8} = m_{31}$$

$$M_g^{9,9} = m_{41}$$

$$M_g^{10,10} = m_{51}$$

All other elements in M_g are zero.

$$M_g^{11,11} = m_{61}$$

$$M_g^{12,12} = m_{71}$$

$$M_g^{13,13} = m_{81}$$

$$M_g^{14,14} = m_{91}$$

$$M_g^{15,15} = m_{10,1}$$

$$M_g^{16,16} = m_{11,1}$$

$$M_g^{17,17} = m_{12,1}$$

$$M_g^{18,18} = m_{13,1}$$

$$M_g^{19,19} = m_{14,1}$$

$$M_g^{20,20} = m_{15,1}$$

$$M_g^{21,21} = m_{16,1}$$

$$M_g^{22,22} = m_{12}$$

$$M_g^{23,23} = J_{12}$$

$$M_g^{24,24} = m_{22}$$

$$M_g^{25,25} = J_{22}$$

$$M_g^{26,26} = m_{32}$$

$$M_g^{27,27} = J_{32}$$

$$T_g^1 = -\sum_{i=1}^{16} S_{i1}$$

$$T_g^2 = \sum_{i=1}^{16} S_{i1} l_{i1}$$

$$T_g^3 = -\sum_{i=1}^{16} S_{i1} w_{i1}$$

$$T_g^4 = -\sum_{i=1}^{6} S_{i2}$$

$$T_g^5 = -\sum_{i=1}^{6} S_{i2} w_{i2}$$

$$T_g^6 = S_{11} - R_{11}$$

$$T_g^7 = S_{21} - R_{21}$$

$$T_g^8 = S_{31} - R_{31}$$

$$T_g^9 = S_{41} - R_{41}$$

$$T_g^{10} = S_{51} - R_{51}$$

$$T_g^{11} = S_{61} - R_{61}$$

$$T_g^{12} = S_{71} - R_{71}$$

$$T_g^{13} = S_{81} - R_{81}$$

$$T_g^{14} = S_{91} - R_{91}$$

$$T_g^{15} = S_{10,1} - R_{10,1}$$

$$T_g^{16} = S_{11,1} - R_{11,1}$$

$$T_g^{17} = S_{12,1} - R_{12,1}$$

$$T_g^{18} = S_{13,1} - R_{13,1}$$

$$T_g^{19} = S_{14,1} - R_{14,1}$$

$$T_g^{20} = S_{15,1} - R_{15,1}$$

$$T_g^{21} = S_{16,1} - R_{16,1}$$

$$T_g^{22} = S_{12} + S_{42} - R_{12} - R_{42}$$

$$T_g^{23} = -\frac{1}{2} w_1 (S_{12} - S_{42}) + \frac{1}{2} w_2 (R_{12} - R_{42})$$

$$T_g^{24} = S_{22} + S_{52} - R_{22} - R_{52}$$

$$T_g^{25} = -\frac{1}{2} w_1 (S_{22} - S_{52}) + \frac{1}{2} w_2 (R_{22} - R_{52})$$

$$T_g^{26} = S_{32} + S_{62} - R_{32} - R_{62}$$

$$T_g^{27} = -\frac{1}{2} w_1 (S_{32} - S_{62}) + \frac{1}{2} w_2 (R_{32} - R_{62})$$

All other elements in T_g are zero.

APPENDIX C : FEM results - first 20 mode shapes

Mode1 : 3.43 [Hz]

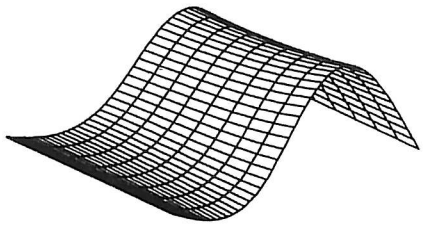

Mode2 : 6.75 [Hz]

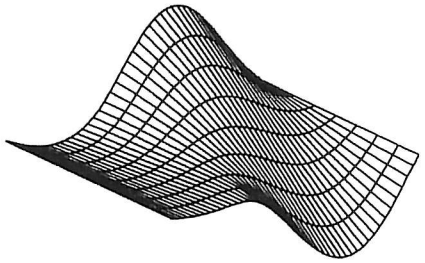

Mode3 : 10.18 [Hz]

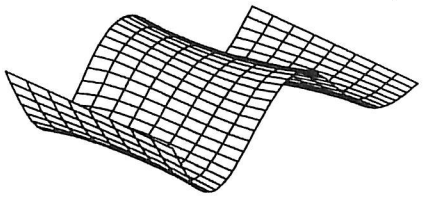

Mode4 : 12.41 [Hz]

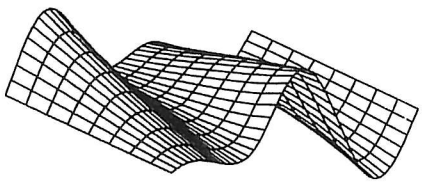

Mode5 : 15.03 [Hz]

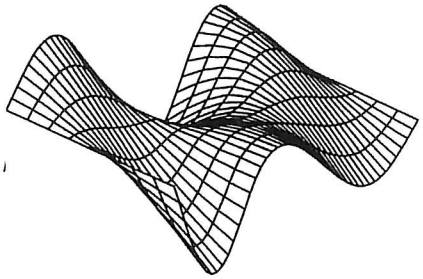

Mode6 : 15.79 [Hz]

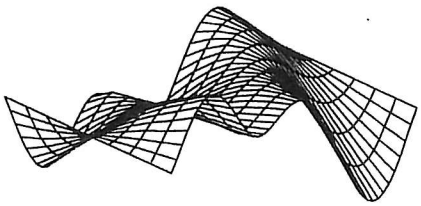

Mode7 : 19.70 [Hz]

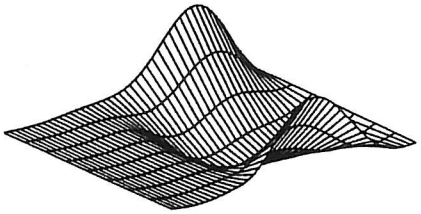

Mode8 : 24.82 [Hz]

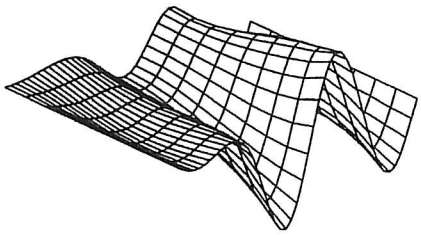

Mode9 : 25.63 [Hz]

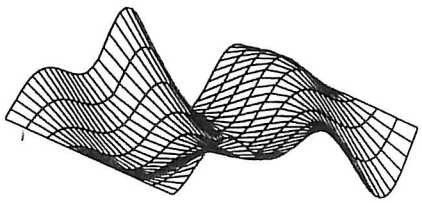

Mode10 : 26.89 [Hz]

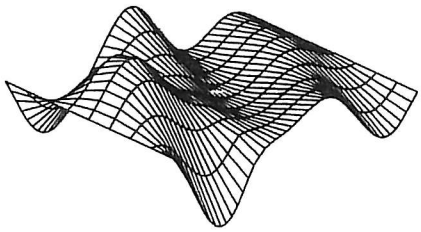

Mode11 : 31.38 [Hz]

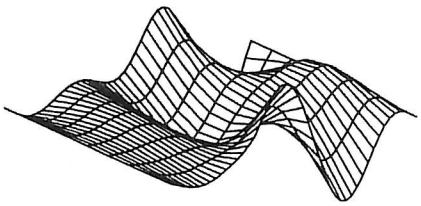

Mode12 : 34.81 [Hz]

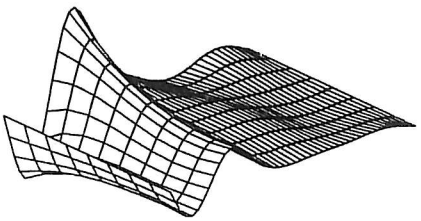

Mode13 : 38.09 [Hz]

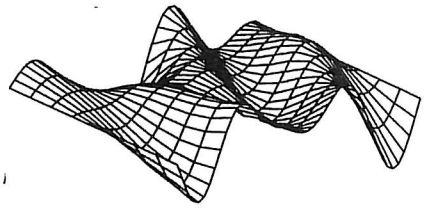

Mode14 : 39.67 [Hz]

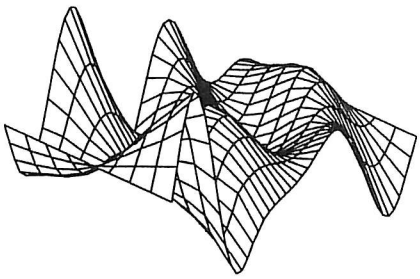

Mode15 : 41.04 [Hz]

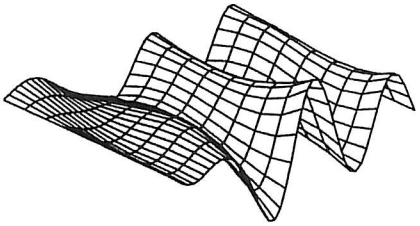

Mode16 : 42.96 [Hz]

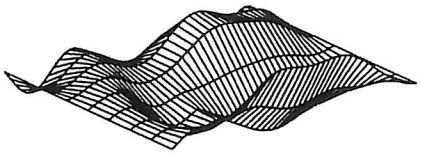

Mode17 : 45.25 [Hz]

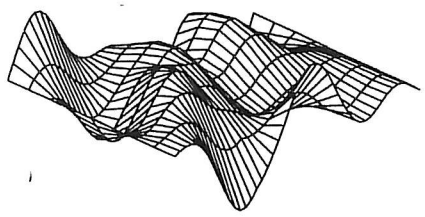

Mode18 : 47.34 [Hz]

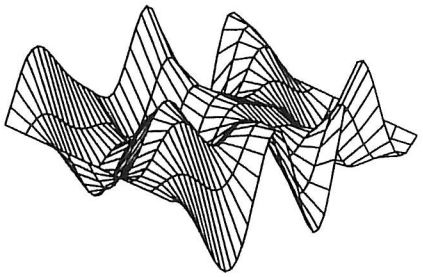

Mode19 : 51.91 [Hz]

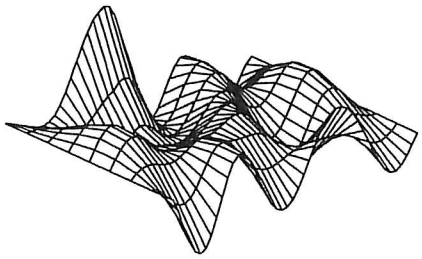

Mode20 : 53.42 [Hz]

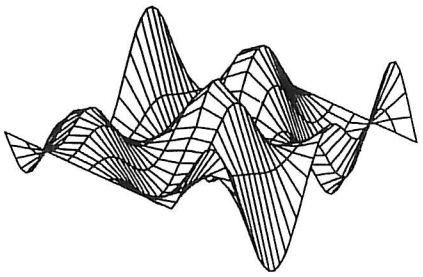

STRUCTURAL RELIABILITY THEORY SERIES

PAPER NO. 144: S. Engelund: *Probabilistic Models and Computational Methods for Chloride Ingress in Concrete.* Ph.D.-Thesis. ISSN 1395-7953 R9707.

PAPER NO. 145: H. U. Köylüoğlu, S. R. K. Nielsen, Jamison Abbott & A. Ş. Çakmak: *Local and Modal Damage Indicators for Reinforced Concrete Shear Frames subject to Earthquakes.* ISSN 0902-7513 R9521

PAPER NO. 146: P. H. Kirkegaard, S. R. K. Nielsen, R. C. Micaletti & A. Ş. Çakmak: *Identification of a Maximum Softening Damage Indicator of RC-Structures using Time-Frequency Techniques.* ISSN 0902-7513 R9522.

PAPER NO. 147: R. C. Micaletti, A. Ş. Çakmak, S. R. K. Nielsen & P. H. Kirkegaard: *Construction of Time-Dependent Spectra using Wavelet Analysis for Determination of Global Damage.* ISSN 0902-7513 R9517.

PAPER NO. 148: H. U. Köylüoğlu, S. R. K. Nielsen & A. Ş. Çakmak: *Hysteretic MDOF Model to Quantify Damage for TC Shear Frames subject to Earthquakes.* ISSN 1395-7953 R9601.

PAPER NO. 149: P. S. Skjærbæk, S. R. K. Nielsen & A. Ş. Çakmak: *Damage Location of Severely Damaged RC-Structures based on Measured Eigenperiods from a Single Response.* ISSN 0902-7513 R9518.

PAPER NO. 150: S. R. K. Nielsen & H. U. Köylüoğlu: *Path Integration applied to Structural Systems with Uncertain Properties.* ISSN 1395-7953 R9602.

PAPER NO. 151: H. U. Köylüoğlu & S. R. K. Nielsen: *System Dynamics and Modified Cumulant Neglect Closure Schemes.* ISSN 1395-7953 R9603.

PAPER NO. 152: R. C. Micaletti, A. Ş. Çakmak, S. R. K. Nielsen, H. U. Köylüoğlu: *Approximate Analytical Solution for the 2nd-Order moments of a SDOF Hysteretic Oscillator with Low Yield Levels Excited by Stationary Gaussian White Noise.* ISSN 1395-7953 R9715.

PAPER NO. 153: R. C. Micaletti, A. Ş. Çakmak, S. R. K. Nielsen & H. U. Köylüoğlu: *A Solution Method for Linear and Geometrically Nonlinear MDOF Systems with Random Properties subject to Random Excitation.* ISSN 1395-7953 R9632.

PAPER NO. 154: J. D. Sørensen, M. H. Faber, I. B. Kroon: *Optimal Reliability-Based Planning of Experiments for POD Curves.* ISSN 1395-7953 R9542.

PAPER NO. 155: J. D. Sørensen, S. Engelund: *Stochastic Finite Elements in Reliability-Based Structural Optimization.* ISSN 1395-7953 R9543.

PAPER NO. 156: C. Pedersen, P. Thoft-Christensen: *Guidelines for Interactive Reliability-Based Structural Optimization using Quasi-Newton Algorithms.* ISSN 1395-7953 R9615.

PAPER NO. 157: P. Thoft-Christensen, F. M. Jensen, C. R. Middleton, A. Blackmore: *Assessment of the Reliability of Concrete Slab Bridges.* ISSN 1395-7953 R9616.

PAPER NO. 158: P. Thoft-Christensen: *Re-Assessment of Concrete Bridges.* ISSN 1395-7953 R9605.

STRUCTURAL RELIABILITY THEORY SERIES

PAPER NO. 159: H. I. Hansen, P. Thoft-Christensen: *Wind Tunnel Testing of Active Control System for Bridges.* ISSN 1395-7953 R9662.

PAPER NO 160: C. Pedersen: *Interactive Reliability-Based Optimization of Structural Systems.* Ph.D.-Thesis. ISSN 1395-7953 R9638.

PAPER NO. 161: S. Engelund, J. D. Sørensen: *Stochastic Models for Chloride-initiated Corrosion in Reinforced Concrete.*ISSN 1395-7953 R9608.

PAPER NO. 162: P. Thoft-Christensen, A. S. Nowak: *Principles of Bridge Reliability - Application to Design and Assessment Codes.* ISSN 1395-7953 R9751.

PAPER NO. 163: P. Thoft-Christensen, F.M. Jensen, C. Middleton, A. Blackmore: *Revised Rules for Concrete Bridges.* ISSN 1395-7953 R9752.

PAPER NO. 164: P. Thoft-Christensen: *Bridge Management Systems. Present and Future.* ISSN 1395-7953 R9711.

PAPER NO. 165: P. H. Kirkegaard, F. M. Jensen, P. Thoft-Christensen: *Modelling of Surface Ships using Artificial Neural Networks.* ISSN 1593-7953 R9625.

PAPER NO. 166: S. R. K. Nielsen, S. Krenk: *Stochastic Response of Energy Balanced Model for Wortex-Induced Vibration.* ISSN 1395-7953 R9710.

PAPER NO. 167: S.R.K. Nielsen, R. Iwankiewicz: *Dynamic systems Driven by Non-Poissonian Impulses: Markov Vector Approach.* ISSN 1395-7953 R9705.

PAPER NO. 168: P. Thoft-Christensen: *Lifetime Reliability Assessment of Concrete Slab Bridges.* ISSN 1395-7953 R9717.

PAPER NO. 169: P. H. Kirkegaard, S. R. K. Nielsen, I. Enevoldsen: *Heavy Vehicles on Minor Highway Bridges - A Literature Review.* ISSN 1395-7953 R9719.

PAPER NO. 170: S.R.K. Nielsen, P.H. Kirkegaard, I. Enevoldsen: *Heavy Vehicles on Minor Highway Bridges - Stochastic Modelling of Surface Irregularities.* ISSN 1395-7953 R9720.

PAPER NO. 171: P. H. Kirkegaard, S. R. K. Nielsen, I. Enevoldsen: *Heavy Vehicles on Minor Highway Bridges - Dynamic Modelling of Vehicles and Bridges.* ISSN 1395-7953 R9721.

PAPER NO. 172: P. H. Kirkegaard, S. R. K. Nielsen, I. Enevoldsen: *Heavy Vehicles on Minor Highway Bridges - Calculation of Dynamic Impact Factors from Selected Crossing Scenarios.* ISSN 1395-7953 R9722.

PAPER NO. 175: C. Frier, J.D. Sørensen: *Stochastic Properties of Plasticity Based Constitutive Law for Concrete.* ISSN 1395-7953 R9727.

PAPER NO. 177: P. Thoft-Christensen: *Review of Industrial Applications of Structural Reliability Theory.* ISSN 1395-7953 R9750.

Department of Building Technology and Structural Engineering
Aalborg University, Sohngaardsholmsvej 57, DK 9000 Aalborg
Telephone: +45 9635 8080 Telefax: +45 9814 8243